CLEO CONF95-1
EPS0192
June 30, 1995

First Observation of the Decay $\tau^- \to K^- \eta \nu_\tau$

B. Barish,[1] M. Chadha,[1] S. Chan,[1] D.F. Cowen,[1] G. Eigen,[1] J.S. Miller,[1] C. O'Grady,[1] J. Urheim,[1] A.J. Weinstein,[1] F. Würthwein,[1] D.M. Asner,[2] M. Athanas,[2] D.W. Bliss,[2] W.S. Brower,[2] G. Masek,[2] H.P. Paar,[2] J. Gronberg,[3] C.M. Korte,[3] R. Kutschke,[3] S. Menary,[3] R.J. Morrison,[3] S. Nakanishi,[3] H.N. Nelson,[3] T.K. Nelson,[3] C. Qiao,[3] J.D. Richman,[3] D. Roberts,[3] A. Ryd,[3] H. Tajima,[3] M.S. Witherell,[3] R. Balest,[4] K. Cho,[4] W.T. Ford,[4] M. Lohner,[4] H. Park,[4] P. Rankin,[4] J.G. Smith,[4] J.P. Alexander,[5] C. Bebek,[5] B.E. Berger,[5] K. Berkelman,[5] K. Bloom,[5] T.E. Browder,[5*] D.G. Cassel,[5] H.A. Cho,[5] D.M. Coffman,[5] D.S. Crowcroft,[5] M. Dickson,[5] P.S. Drell,[5] D.J. Dumas,[5] R. Ehrlich,[5] R. Elia,[5] P. Gaidarev,[5] R.S. Galik,[5] M. Garcia-Sciveres,[5] B. Gittelman,[5] S.W. Gray,[5] D.L. Hartill,[5] B.K. Heltsley,[5] S. Henderson,[5] C.D. Jones,[5] S.L. Jones,[5] J. Kandaswamy,[5] N. Katayama,[5] P.C. Kim,[5] D.L. Kreinick,[5] T. Lee,[5] Y. Liu,[5] G.S. Ludwig,[5] J. Masui,[5] J. Mevissen,[5] N.B. Mistry,[5] C.R. Ng,[5] E. Nordberg,[5] J.R. Patterson,[5] D. Peterson,[5] D. Riley,[5] A. Soffer,[5] P. Avery,[6] A. Freyberger,[6] K. Lingel,[6] C. Prescott,[6] J. Rodriguez,[6] S. Yang,[6] J. Yelton,[6] G. Brandenburg,[7] D. Cinabro,[7] T. Liu,[7] M. Saulnier,[7] R. Wilson,[7] H. Yamamoto,[7] T. Bergfeld,[8] B.I. Eisenstein,[8] J. Ernst,[8] G.E. Gladding,[8] G.D. Gollin,[8] M. Palmer,[8] M. Selen,[8] J.J. Thaler,[8] K.W. Edwards,[9] K.W. McLean,[9] M. Ogg,[9] A. Bellerive,[10] D.I. Britton,[10] E.R.F. Hyatt,[10] R. Janicek,[10] D.B. MacFarlane,[10] P.M. Patel,[10] B. Spaan,[10] A.J. Sadoff,[11] R. Ammar,[12] P. Baringer,[12] A. Bean,[12] D. Besson,[12] D. Coppage,[12] N. Copty,[12] R. Davis,[12] N. Hancock,[12] S. Kotov,[12] I. Kravchenko,[12] N. Kwak,[12] Y. Kubota,[13] M. Lattery,[13] M. Momayezi,[13] J.K. Nelson,[13] S. Patton,[13] R. Poling,[13] V. Savinov,[13] S. Schrenk,[13] R. Wang,[13] M.S. Alam,[14] I.J. Kim,[14] Z. Ling,[14] A.H. Mahmood,[14] J.J. O'Neill,[14] H. Severini,[14] C.R. Sun,[14] F. Wappler,[14] G. Crawford,[15] R. Fulton,[15] D. Fujino,[15] K.K. Gan,[15] K. Honscheid,[15] H. Kagan,[15] R. Kass,[15] J. Lee,[15] M. Sung,[15] A. Undrus,[15 †] C. White,[15] A. Wolf,[15] M.M. Zoeller,[15] X. Fu,[16] B. Nemati,[16] W.R. Ross,[16] P. Skubic,[16] M. Wood,[16] M. Bishai,[17] J. Fast,[17] E. Gerndt,[17] J.W. Hinson,[17] T. Miao,[17] D.H. Miller,[17] M. Modesitt,[17] E.I. Shibata,[17] I.P.J. Shipsey,[17] P.N. Wang,[17] L. Gibbons,[18] S.D. Johnson,[18] Y. Kwon,[18] S. Roberts,[18] E.H. Thorndike,[18] T.E. Coan,[19] J. Dominick,[19] V. Fadeyev,[19] I. Korolkov,[19] M. Lambrecht,[19] S. Sanghera,[19] V. Shelkov,[19] T. Skwarnicki,[19] R. Stroynowski,[19] I. Volobouev,[19] G. Wei,[19] M. Artuso,[20] M. Gao,[20] M. Goldberg,[20] D. He,[20] N. Horwitz,[20] S. Kopp,[20] G.C. Moneti,[20] R. Mountain,[20] F. Muheim,[20] Y. Mukhin,[20] S. Playfer,[20] S. Stone,[20] X. Xing,[20] J. Bartelt,[21] S.E. Csorna,[21] V. Jain,[21] S. Marka,[21] D. Gibaut,[22] K. Kinoshita,[22] and P. Pomianowski[22]

(CLEO Collaboration)

[1]*California Institute of Technology, Pasadena, California 91125*
[2]*University of California, San Diego, La Jolla, California 92093*
[3]*University of California, Santa Barbara, California 93106*
[4]*University of Colorado, Boulder, Colorado 80309-0390*
[5]*Cornell University, Ithaca, New York 14853*
[6]*University of Florida, Gainesville, Florida 32611*
[7]*Harvard University, Cambridge, Massachusetts 02138*
[8]*University of Illinois, Champaign-Urbana, Illinois, 61801*
[9]*Carleton University, Ottawa, Ontario K1S 5B6 and the Institute of Particle Physics, Canada*
[10]*McGill University, Montréal, Québec H3A 2T8 and the Institute of Particle Physics, Canada*
[11]*Ithaca College, Ithaca, New York 14850*
[12]*University of Kansas, Lawrence, Kansas 66045*
[13]*University of Minnesota, Minneapolis, Minnesota 55455*
[14]*State University of New York at Albany, Albany, New York 12222*
[15]*Ohio State University, Columbus, Ohio, 43210*
[16]*University of Oklahoma, Norman, Oklahoma 73019*
[17]*Purdue University, West Lafayette, Indiana 47907*
[18]*University of Rochester, Rochester, New York 14627*
[19]*Southern Methodist University, Dallas, Texas 75275*
[20]*Syracuse University, Syracuse, New York 13244*
[21]*Vanderbilt University, Nashville, Tennessee 37235*
[22]*Virginia Polytechnic Institute and State University, Blacksburg, Virginia, 24061*

The decay of the τ lepton into a charged hadron, an η meson plus a neutrino has been observed for the first time using the CLEO II detector. The measured branching fraction is $B(\tau^- \to h^- \eta \nu_\tau) = (2.4 \pm 0.8 \pm 0.4 \pm 0.1) \times 10^{-4}$. The uncertainties shown are statistical, systematic and theoretical model dependence. By identifying the charged hadron, the exclusive branching fractions are $B(\tau^- \to K^- \eta \nu_\tau) = (2.6 \pm 0.5 \pm 0.3 \pm 0.3) \times 10^{-4}$ and $B(\tau^- \to \pi^- \eta \nu_\tau) < 2.5 \times 10^{-4}$ at 95% confidence level. These results are consistent with the standard model expectations.

*Permanent address: University of Hawaii at Manoa

†Permanent address: BINP, Novosibirsk, Russia

The decays of the τ lepton involving η mesons are suppressed in comparison with all-pion decays. The decay [1] $\tau^- \to \pi^- \eta \nu_\tau$ is highly suppressed due to chiral symmetry and is a second class weak current because it violates G-parity conservation. The standard model predicts a branching fraction of $\sim 1.5 \times 10^{-5}$ [2,3]. Since there is no G-parity constraint on the analogous Cabibbo suppressed decay, $\tau^- \to K^- \eta \nu_\tau$, the branching fraction is expected to be higher by an order of magnitude, $\sim (1.2 - 1.6) \times 10^{-4}$ [2,4]. The decays with η and at least two pions can proceed through the chiral anomaly term in the effective lagrangian and hence there is no strong suppression. Previously, CLEO II measured the branching fraction $B(\tau^- \to \pi^- \eta \pi^0 \nu_\tau) = (1.7 \pm 0.2 \pm 0.2) \times 10^{-3}$ [5], and set the following upper limits, $B(\tau^- \to \pi^- \eta \nu_\tau) < 3.4 \times 10^{-4}$ and $B(\tau^- \to K^- \eta \nu_\tau) < 4.7 \times 10^{-4}$ at 95% C.L. Using a four times larger data sample we report in this paper the first measurement of the decay $\tau^- \to K^- \eta \nu_\tau$ and a new upper limit on $\tau^- \to \pi^- \eta \nu_\tau$.

The data used in this analysis were collected with the CLEO II detector [6] from e^+e^- collisions at the Cornell Electron-positron Storage Ring (CESR) at a center-of-mass energy $\sqrt{s} \sim 10.6$ GeV. The total integrated luminosity of the sample is $3.5 fb^{-1}$, corresponding to $\sim 3.2 \times 10^6$ produced $\tau^+\tau^-$ events. CLEO II is a solenoidal spectrometer with a solid angle coverage of 95% of 4π steradians for charged particles and 98% of 4π steradians for photons. The momenta and specific ionization (dE/dx) of charged particles are measured with three cylindrical drift chambers between 5 and 90 cm from the e^+e^- interaction point (IP), with a total of 67 layers. These are surrounded by a scintillation time-of-flight (TOF) system and a CsI(Tl) calorimeter with 7800 crystals. These detector systems are installed inside a 1.5 T superconducting solenoidal magnet, surrounded by proportional tube chambers with iron absorber for muon identification. For hadrons, the dE/dx (TOF) resolution is $\sim 7.1\%$ (154 ps), providing K/π separation of greater than two standard deviation (σ) for particle momenta below 0.75 (1.07) GeV/c. For the relativistic rise region above 2.0 GeV/c, the dE/dx measurement provides $\sim 1.8\sigma$ K/π separation.

Since the particle identification capacity depends on the particle momentum, we use two complementary methods to distinguish $\tau^- \to (K^-/\pi^-)\eta \nu_\tau$. In the first method (Method I), we exclude events with charged particle momenta in the 1.0-2.0 GeV/c range where the K/π separation is limited. Unfortunately, the momentum spectra of the signal decays peak in this region. The second method, Method II, uses the full momentum range. Although the K/π fraction is effectively determined from outside the 1.0-2.0 GeV/c region, this intermediate range is helpful in constraining the sum of these two decay modes. This method improves the detection efficiency and is less dependent on the model for the $h^-\eta$ spectral function. However, this method has a larger systematic error associated with particle identification. Due to the higher detection efficiency, only this method is used to set an upper limit on $B(\tau^- \to \pi^- \eta \nu_\tau)$ and the inclusive branching fraction, $B(\tau^- \to h^- \eta \nu_\tau) = B(\tau^- \to K^- \eta \nu_\tau) + B(\tau^- \to \pi^- \eta \nu_\tau)$. The inclusive branching fraction is measured without using particle identification. Since $B(\tau^- \to \pi^- \eta \nu_\tau)$ is predicted to be smaller than $B(\tau^- \to K^- \eta \nu_\tau)$ by an order of magnitude, this inclusive measurement is expected to be dominated by $B(\tau^- \to K^- \eta \nu_\tau)$. In both methods, we identify η mesons using the decay $\eta \to \gamma\gamma$. To improve the detection efficiency in Method I, we also utilize $\eta \to \pi^+\pi^-\pi^0$, and use a more inclusive tag on the other τ in the event. The two methods yield largely uncorrelated samples of $\tau^- \to K^- \eta \nu_\tau$ candidates, because of the differences in the η reconstruction, the momentum coverage, and the tagging techniques. To minimize the statistical error, results from the two methods are combined for the final result.

Events with two (or four for $\eta \to \pi^+\pi^-\pi^0$) charged tracks are selected, with zero net charge. Each event is divided into two hemispheres using both charged tracks and photons. The momentum vectors of the τ decay products in the two hemispheres must be approximately back-to-back. The tag hemisphere must contain only one charged particle. There must be exactly two well-identified photons in the signal hemisphere. Strict photon counting is important for the suppression of feed-down from $\tau^- \to \pi^-\eta\pi^0\nu_\tau$ decays. The total invariant mass of the particles in each hemisphere must be less than the τ mass. Backgrounds due to two-photon processes are suppressed by the back-to-back cut described previously, and by requiring momentum imbalance in the direction transverse to the beam. In Method II, we further require the tag hemisphere to contain no photons above 70 MeV since $e^+e^- \to q\bar{q}$ backgrounds have higher photon multiplicity. These backgrounds and the two-photon backgrounds are further suppressed by a cut on the missing mass: $0.5 < M_m < 6.5$ GeV/c^2.

Kaon (pion) candidates are identified using dE/dx and TOF information. In Method I, the dE/dx measurement must be within 2σ of that expected for a kaon (pion) for $0.2 < p < 1.0$ GeV/c, and $< 1\sigma$ for $2.0 < p < 4.5$ GeV/c. For $p < 1.0$ GeV/c, if good TOF information is available [7], the TOF must be within 2σ of that expected for a kaon (pion) and greater than 3σ away from that for a pion (kaon). In addition, for $p > 0.4$ GeV/c, good TOF information must be available. In Method II, we cut on the chi-square difference between the kaon and pion hypotheses using dE/dx and TOF (if available): $\chi^2_K - \chi^2_\pi$. A kaon (pion) rich sample is obtained by requiring $\chi^2_K - \chi^2_\pi < 0$ (> 0). Since both $\tau^- \to K^-\eta\nu_\tau$ and $\pi^-\eta\nu_\tau$ decays contribute to both sub-samples we obtained the branching fractions for each of these modes by unfolding the observed yields.

The two-photon invariant mass spectra normalized with respect to the mass resolution, $S_{\gamma\gamma} = \frac{M_{\gamma\gamma}-M_\eta}{\sigma_{\gamma\gamma}}$, are shown in Fig. 1 for Method II. In Fig. 1a where there is no particle identification requirement, a significant η signal is observed. The curves show fits to the data using a Gaussian with a low-mass tail representing the η signal over a polynomial background. The signal shape is constrained to the Monte Carlo expectation. After application of the particle identification requirement, we find that the observed η's are preferentially accompanied by a kaon, as illustrated in Fig. 1b,c. The complementary Method I also yields a significant η signal associated with kaons using both $\eta \to \gamma\gamma$ (Fig. 2) and $\eta \to \pi^+\pi^-\pi^0$ (Fig. 3) decay modes. The event yields from the fits are shown in Table I. The predictions for the detection efficiencies and backgrounds are also shown.

The detection efficiency is calculated using a Monte Carlo simulation. The KORALB program is used to generate $\tau^+\tau^-$ pairs according to the standard electroweak theory, including α^3 radiative corrections [8]. The decays $\tau^- \to K^-\eta\nu_\tau$ ($\pi^-\eta\nu_\tau$) are modeled assuming a $V - A$ weak interaction with either a phase space distribution for the $h^-\eta$ system or a $K^*(1410)$ ($a_0(980)$) resonance. The detection efficiencies are taken to be the average between these two models. The difference serves an estimate of the model dependence. The detector response is simulated using the GEANT program [9]. Detector activity not attributable to the e^+e^- interaction is modeled by embedding random trigger events into the generated events.

For Method I, the kaon identification efficiency has been calibrated as a function of momentum using $D^{*+} \to D^0\pi^+ \to K^-\pi^+\pi^+$ decays from the data. The probability for misidentification of a pion as a kaon is calculated empirically as a function of momentum using isolated pions from K_S decays in hadronic events. The calibration agrees with the Monte Carlo simulation to within 4% on efficiency and 20% on misidentification probability. For Method II, we rely on the Monte Carlo simulation.

The hadronic background, $e^+e^- \to q\bar{q}$, is estimated from the data, using events in which the invariant mass in one hemisphere above the τ mass. In Method II, the events are selected with somewhat looser selection criteria in order to increase statistics. The Lund Monte Carlo [10] is used to extrapolate the hadronic background measured with these looser criteria to the nominal τ event selection cuts. In Method I, 1 vs. 3 events from the data selected with a 3-prong jet mass above the τ mass is used to estimate the fraction of hadronic events with the invariant mass in one hemisphere below the τ mass. Feed-down from $\tau^- \to \pi^-\eta\pi^0\nu_\tau$ events is estimated using the Monte Carlo. From a study of cut variations, we conclude that the background from two-photon collisions is negligible. The $K\eta$ invariant mass distribution for events selected with no particle identification is shown in Fig. 4. The background under the η peak has been subtracted using side-bands. The sample is relatively clean as indicated by the small number of events above the τ mass, which is well reproduced by the background estimate. After correcting for the background and detection efficiency, the branching fractions are extracted by normalizing to the luminosity and $\tau^+\tau^-$ cross section. The branching fractions obtained are shown in Table I.

There are several sources of systematic errors as shown in Table II. The systematic error in the detection efficiency due to the uncertainty in the simulation of photons and hadronic interactions is estimated by varying the photon selection criteria. The systematic error in the hadronic background calculation is dominated by the statistical error due to the paucity of events with high invariant mass. The branching fractions have also been measured with an electron or muon tag, for which the background is negligible; these measurements are consistent with the results from the generic tags. The systematic error due to the imperfection of the trigger simulation was studied by comparing the results with those which require at least two trigger lines being satisfied [11]. In Method I, the uncertainty in the K identification efficiency is due to the limited sample of D^* events used in the calibration of that efficiency. The uncertainty in the misidentification background from pions includes the statistical error due to the limited sample of misidentified pions from K_S. In Method II, the particle identification systematics was determined by varying the $\chi^2_K - \chi^2_\pi$ cut. Other systematic errors listed include the uncertainties in the luminosity, $\tau^+\tau^-$ cross section, and the branching fractions of $\eta \to \gamma\gamma$ and $\pi^+\pi^-\pi^0$.

In Method I, the branching fractions for $\tau^- \to K^-\eta\nu_\tau$ obtained with $\eta \to \gamma\gamma$ and $\eta \to \pi^+\pi^-\pi^0$ agree within the statistical errors. The average of these two decay modes is $(3.1 \pm 0.9 \pm 0.6 \pm 0.5) \times 10^{-4}$, where the first error is statistical, the second is systematic, and the third is the model dependence [13]. The statistical overlap between this sample and that from Method II is small; the correlation coefficient is +11%. Taking this correlation into account, the results from the two methods differ by $(0.8 \pm 1.0) \times 10^{-4}$ (statistical error only). Thus, the two methods yield consistent results. After accounting for the correlation, the branching fraction averaged over the two methods is

$$B(\tau^- \to K^-\eta\nu_\tau) = (2.6 \pm 0.5 \pm 0.3 \pm 0.3) \times 10^{-4}.$$

This is consistent with the inclusive measurement with no identification cuts,

$$B(\tau^- \to h^-\eta\nu_\tau) = (2.4 \pm 0.8 \pm 0.4 \pm 0.1) \times 10^{-4},$$

indicating that $B(\tau^- \to K^-\eta\nu_\tau)$ is much larger than $B(\tau^- \to \pi^-\eta\nu_\tau)$ as predicted. To obtain an upper limit on the latter contribution, we combine in quadrature the statistical and additive systematic errors, including the model dependent error. The limit is then loosened by one unit of multiplicative systematical error. The resulting upper limit at 95% C.L. is:

$$B(\tau^- \to \pi^-\eta\nu_\tau) < 2.5 \times 10^{-4}.$$

In summary, we have measured for the first time the branching fraction of $\tau^- \to K^-\eta\nu_\tau$ and set a more stringent limit on $B(\tau^- \to \pi^-\eta\nu_\tau)$. The results are consistent with the theoretical predictions.

ACKNOWLEDGEMENTS

We gratefully acknowledge the effort of the CESR staff in providing us with excellent luminosity and running conditions. This work was supported by the National Science Foundation, the U.S. Department of Energy, the Heisenberg Foundation, the Alexander von Humboldt Stiftung, the Natural Sciences and Engineering Research Council of Canada, and the A.P. Sloan Foundation.

---

[1] In this paper, charge conjugate states are implied.

[2] A. Pich, Phys. Lett. **196B**, 561 (1987).

[3] A. Bramon, S. Narison, A. Pich, Phys. Lett. **196B**, 543 (1987); C.K. Zachos, Y. Meurice, Mod. Phys. Lett. **A2**, 247 (1987); N. Paver, D. Treleani, Nuovo Cim. Lett. **31**, 364 (1981).

[4] G. J. Aubrecht II, N. Chahrouri, K. Slanec, Phys. Rev. **D24**, 1318 (1981).

[5] M. Artuso *et al.*, Phys. Rev. Lett. **69**, 3278 (1992).

[6] Y. Kubota *et al.*, Nucl. Inst. and Meth. **A320**, 66 (1992).

[7] The requirements on TOF, such as minimum pulse height, reduce the detection efficiency by $\sim 20\%$.

[8] S. Jadach and Z. Was, Comp. Phys. Comm. **36**, 191 (1985); *ibid.* **64**, 267 (1991); S. Jadach, J. H. Kuhn, and Z. Was, *ibid.* **64**, 275 (1991).

[9] R. Brun *et al.*, CERN Report No. CERN-DD/EE/84-1, 1987 (unpublished).

[10] T. Sjostrand and M. Bengtsson, Comp. Phys. Comm. **43**, 367 (1987).

[11] M. Battle *et al.*, Phys. Rev. Lett. **73**, 1079 (1994).

[12] Review of Particle Properties, L. Montanet *et al.*, Phy. Rev. **D50**, (1994).

[13] The branching fractions for the K^* resonance model can be obtained by shifting down the measured branching fractions by one unit of the third error.

TABLE I. Summary of signals, backgrounds, efficiencies, and branching fractions. All errors are statistical, except for the errors on efficiencies which reflect the model dependence.

	$h^-\eta$	$K^-\eta$	$K^-\eta$	$K^-\eta$	$\pi^-\eta$
η decay	$\gamma\gamma$	$\gamma\gamma$	$\gamma\gamma$	$\pi^+\pi^-\pi^0$	$\gamma\gamma$
Method	II	II	I	I	II
Data	57 ± 13	35 ± 8	27 ± 8	19 ± 6	23 ± 10
$\pi^-\eta\pi^0$ feed-down	4.4 ± 1.0	0.7 ± 0.3	0.4 ± 0.2	1.2 ± 0.4	3.4 ± 0.8
$e^+e^- \to q\bar{q}$	11.7 ± 6.0	2.0 ± 1.7	4.8 ± 2.8	1.8 ± 1.3	9.8 ± 5.1
Efficiency (%)	7.0 ± 0.4	5.7 ± 0.4	3.2 ± 0.6	2.4 ± 0.2	5.2 ± 0.2
Cross-feed efficiency (%)	—	0.9 ± 0.1	0.7 ± 0.1	0.5 ± 0.1	1.3 ± 0.1
Cross-feed (events)	—	0.5 ± 2.0	0.3 ± 1.5	0.2 ± 0.7	7.5 ± 2.1
$B(10^{-4})$	2.4 ± 0.8	2.3 ± 0.6	2.7 ± 1.0	4.3 ± 1.7	0.2 ± 0.9

TABLE II. Summary of systematic errors. For the $\pi^-\eta$ mode, numbers with the 10^{-4} factor indicate additive systematic errors in absolute units. All other numbers are relative errors in percent.

	$h^-\eta$	$K^-\eta$	$K^-\eta$	$K^-\eta$	$\pi^-\eta$
η decay	$\gamma\gamma$	$\gamma\gamma$	$\gamma\gamma$	$\pi^+\pi^-\pi^0$	$\gamma\gamma$
Method	II	II	I	I	II
Luminosity	2	2	2	2	2
Cross section	1	1	1	1	1
η BR [12]	1	1	1	3	1
K/π (mis)identification	–	13	5	5	0.3×10^{-4}
Background	14	12	13	10	0.7×10^{-4}
Fitting	5	5	5	5	5
Trigger	3	3	3	3	3
Photon detection	9	9	9	9	9
MC statistics	4	4	4	4	4
Total	18	21	18	16	0.8×10^{-4} and 12%
Spectral function	5	7	19	7	0.2×10^{-4}

FIG. 1. The $\gamma\gamma$ invariant mass spectrum obtained from Method II for candidates of the decay (a) $\tau^- \to h^- \eta \nu_\tau$ (no particle identification cuts), (b) $\tau^- \to K^- \eta \nu_\tau$, (c) $\tau^- \to \pi^- \eta \nu_\tau$. The mass is expressed in standard deviations from the nominal η mass.

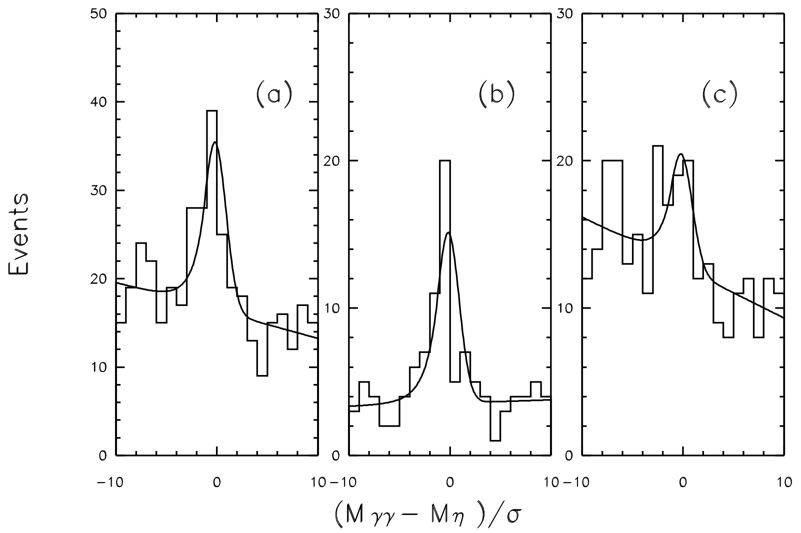

FIG. 2. The $\gamma\gamma$ invariant mass spectrum obtained from Method I for candidates of the decay $\tau^- \to K^- \eta \nu_\tau$. The mass is expressed in standard deviations from the nominal η mass.

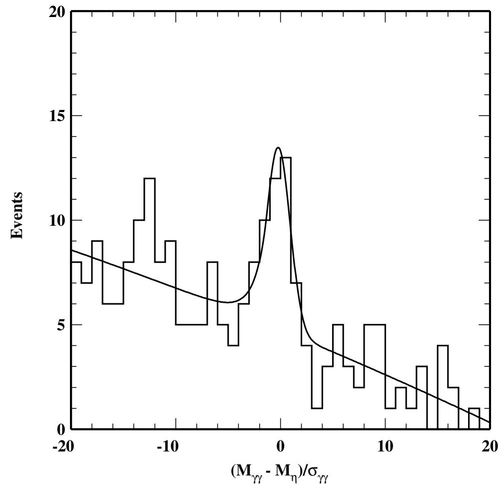

FIG. 3. The $\pi^+\pi^-\pi^0$ invariant mass spectrum. The charged hadron accompanying the three pions is identified as a K candidate.

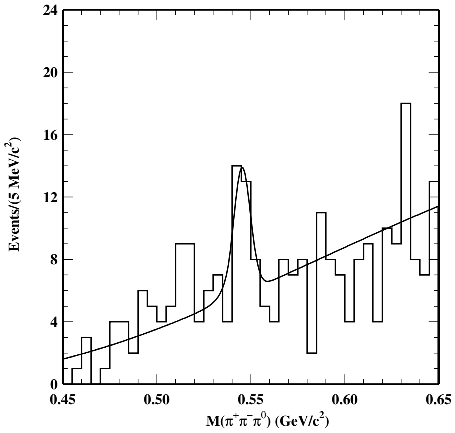

FIG. 4. The $K\eta$ invariant mass for events selected with no particle identification cuts. The η sideband has been subtracted. (a) The data without the background corrections. The background expectation for $e^+e^- \rightarrow q\bar{q}$ is shown as a solid line and $\tau^- \rightarrow \pi^-\eta\pi^0\nu_\tau$ as a dashed line. (b) The data after background corrections. The solid line represents the $V - A$ interaction with a $K^-\eta$ phase space spectral function, whereas the dashed line corresponds to a $K_1^*(1410)$ resonance.